

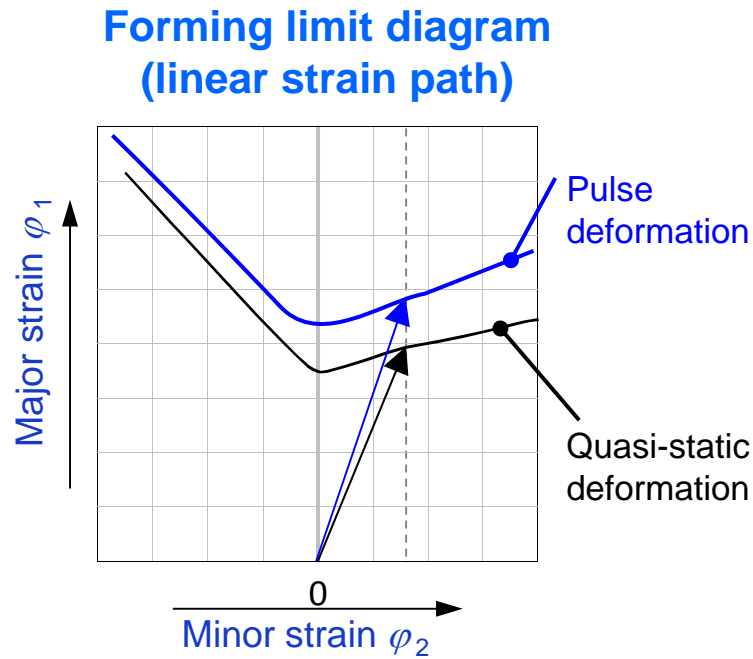
Design of new technologies for the numerical simulation of combined quasi-static dynamic forming processes

Y. Kiliclar, I. N. Vladimirov, S. Wulfinghoff & S. Reese

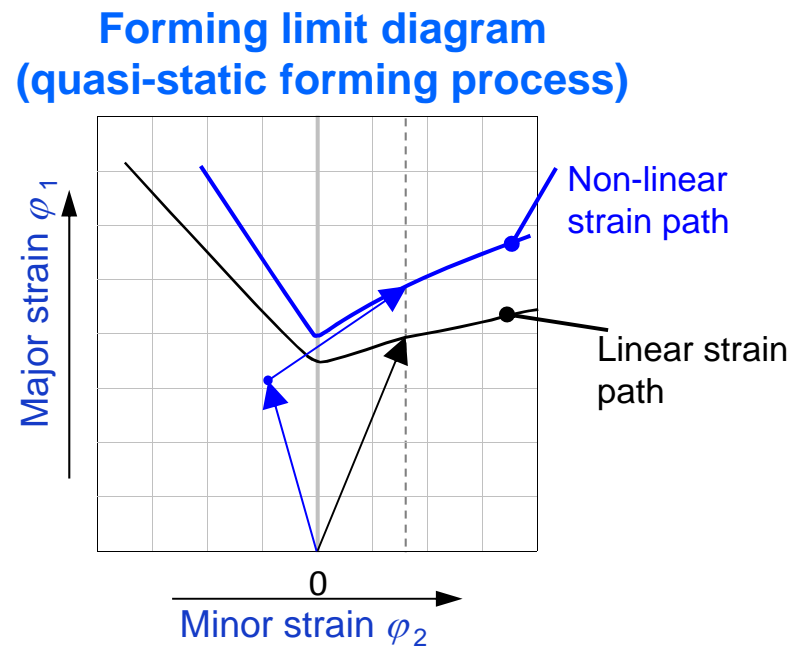
- A. Motivation
- B. Material modelling
- C. Parameter identification
- D. Validation
- E. Conclusion/Outlook

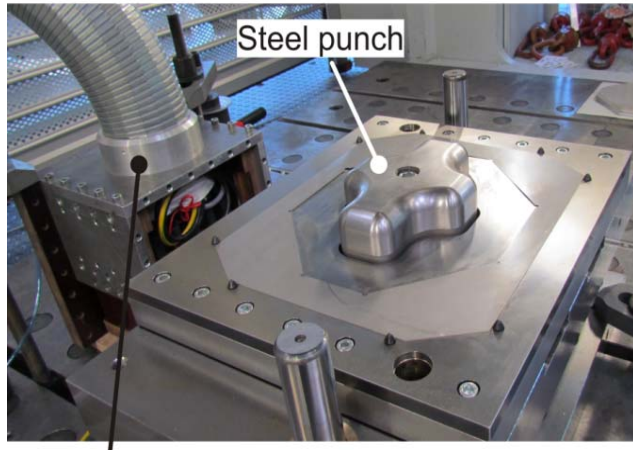


High **strain rate** (pulse forming) can shift the forming limit



Change in the **strain path** can shift the forming limit

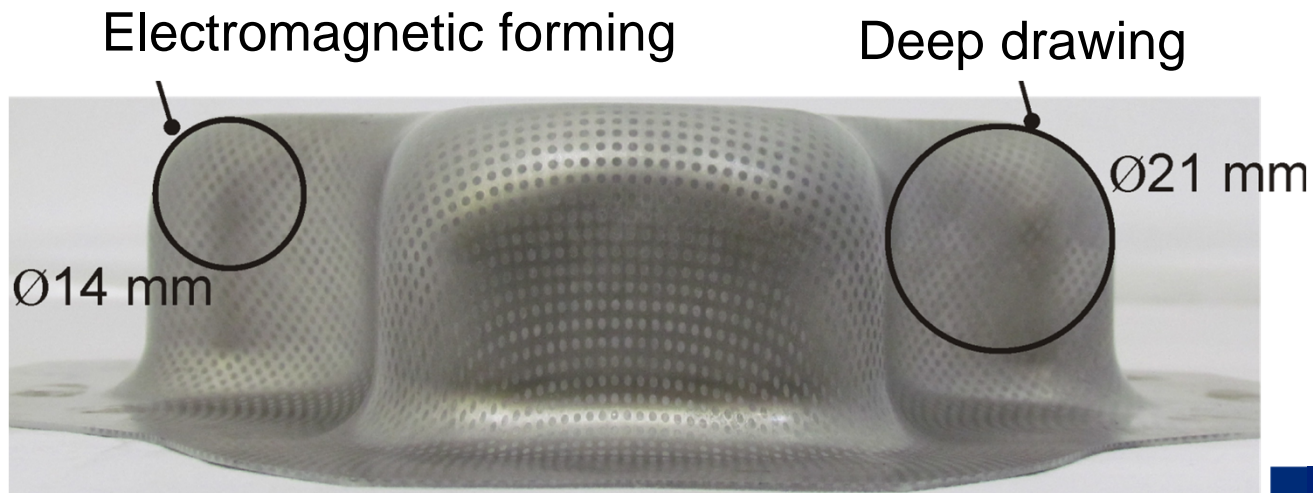




Interface to capacitor



Coil windings



Electromagnetic forming

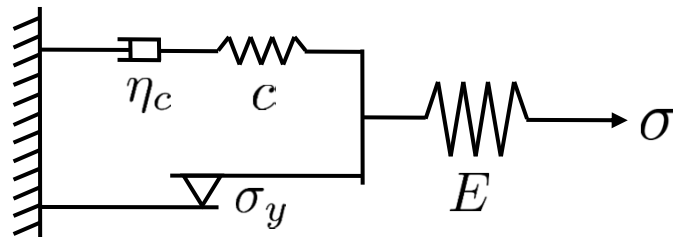
Deep drawing

$\text{\O}14 \text{ mm}$

$\text{\O}21 \text{ mm}$



- Starting point:
Elastoplasticity with nonlinear isotropic / kinematic hardening
(„pseudo viscosity“)

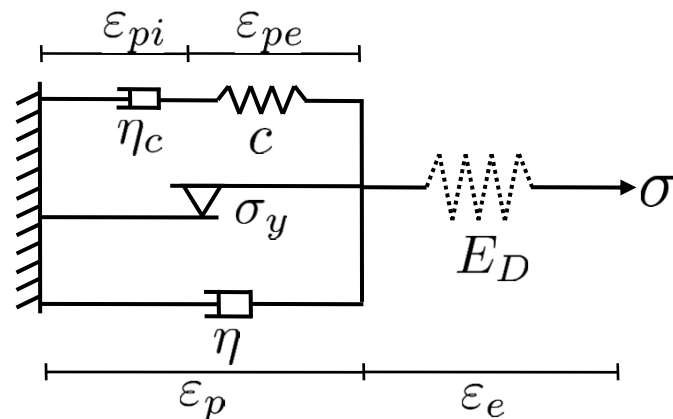


- Rate-independent:

$$“\eta_c” = \frac{c}{\dot{\lambda} b}$$

Vladimirov et al. 2008
Dettmer & Reese 2004

- Model extension:
Damage coupled viscoplasticity with nonlinear isotropic / kinematic hardening



- Effective stress:

Rabotnov 1968

$$\tilde{\sigma} = \frac{\sigma}{1 - D} = E \varepsilon_e$$

$$E_D = E (1 - D)$$

- Rate-dependent:

$$\dot{\lambda} = \frac{\langle \Phi \rangle^m}{\eta}$$

multiplicative split:

$$\mathbf{F} = \mathbf{F}_e \mathbf{F}_p, \quad \mathbf{F}_p = \mathbf{F}_{p_e} \mathbf{F}_{p_i}$$

Lion 2000

Helmholtz free energy:

$$\psi = \psi_e(\mathbf{C}_e) + \psi_{kin}(\mathbf{C}_{p_e}) + \psi_{iso}(\kappa)$$

kinematic hardening

isotropic hardening

$$\mathbf{C}_e = \mathbf{F}_e^T \mathbf{F}_e = \mathbf{F}_p^{-T} \mathbf{C} \mathbf{F}_p^{-1}, \quad \mathbf{C}_{p_e} = \mathbf{F}_{p_e}^T \mathbf{F}_{p_e} = \mathbf{F}_{p_i}^{-T} \mathbf{C}_p \mathbf{F}_{p_i}^{-1}$$

Clausius-Duhem inequality (isothermal processes):

$$-\dot{\psi} + \mathbf{S} \cdot \frac{1}{2} \dot{\mathbf{C}} \geq 0$$

$$\left(\mathbf{S} - 2\mathbf{F}_p^{-1} \frac{\partial \psi_e}{\partial \mathbf{C}_e} \mathbf{F}_p^{-T} \right) \cdot \frac{1}{2} \dot{\mathbf{C}} + \underbrace{(\mathbf{M} - \boldsymbol{\chi})}_{:=\boldsymbol{\Sigma}} \cdot \mathbf{d}_p + \mathbf{M}_{kin} \cdot \mathbf{d}_{p_i} + R \dot{\kappa} + Y \dot{D} \geq 0$$

$$\mathbf{d}_p = \dot{\lambda} \frac{\partial \Phi}{\partial \Sigma}$$

plastic flow rule

Vladimirov et al. 2011

$$\mathbf{d}_{p_i} = \dot{\lambda} \frac{b}{c} \mathbf{M}_{kin}^D$$

symmetric internal variables!

kinematic hardening

$$\dot{\kappa} = \dot{\lambda} \frac{\partial \Phi}{\partial R}, \quad R = -Q (1 - e^{-\beta \kappa})$$

isotropic hardening

$$\dot{D} = \dot{\lambda} \sqrt{\frac{2}{3}} \frac{1}{1-D} \left(\frac{Y}{s} \right)^k H(\kappa - p_D)$$

damage Lemaitre (1992)

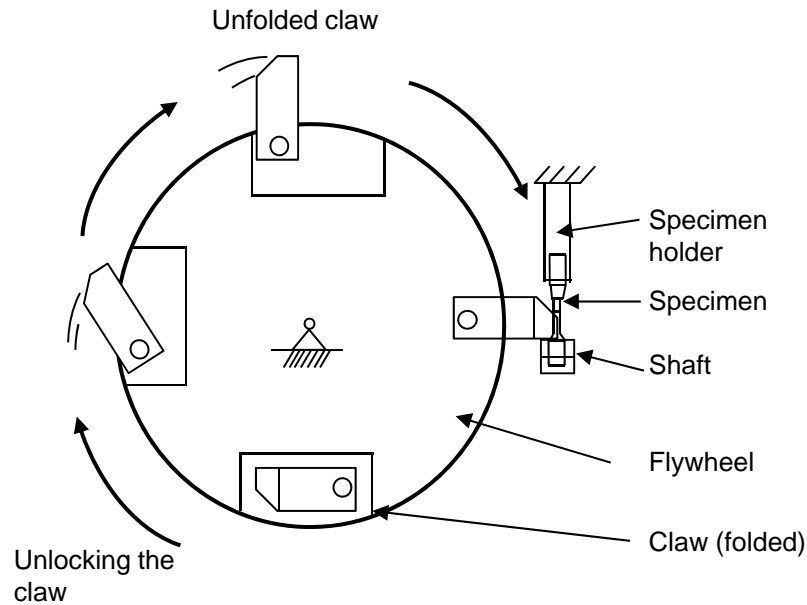
$$\Phi = \sqrt{\Sigma^D \cdot (\tilde{A}[\Sigma^D])} - \sqrt{\frac{2}{3}} (\sigma_y - R)$$

yield function (anisotropy)

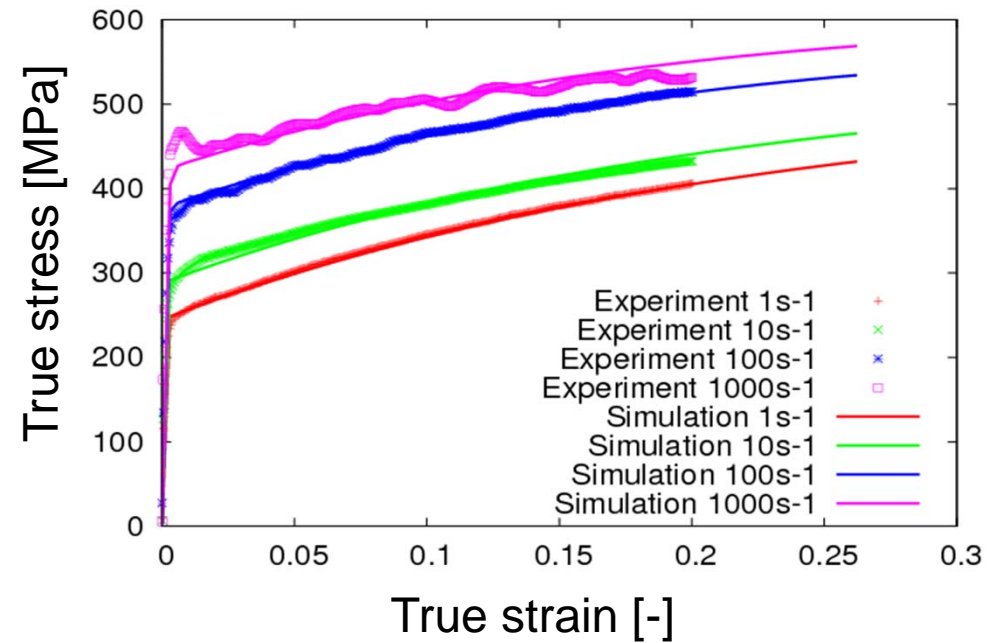
$$\dot{\lambda} = \frac{\langle \Phi \rangle^m}{\eta}$$

Perzyna formulation

Pull-back to reference configuration!



Flow curves for varying strain rates

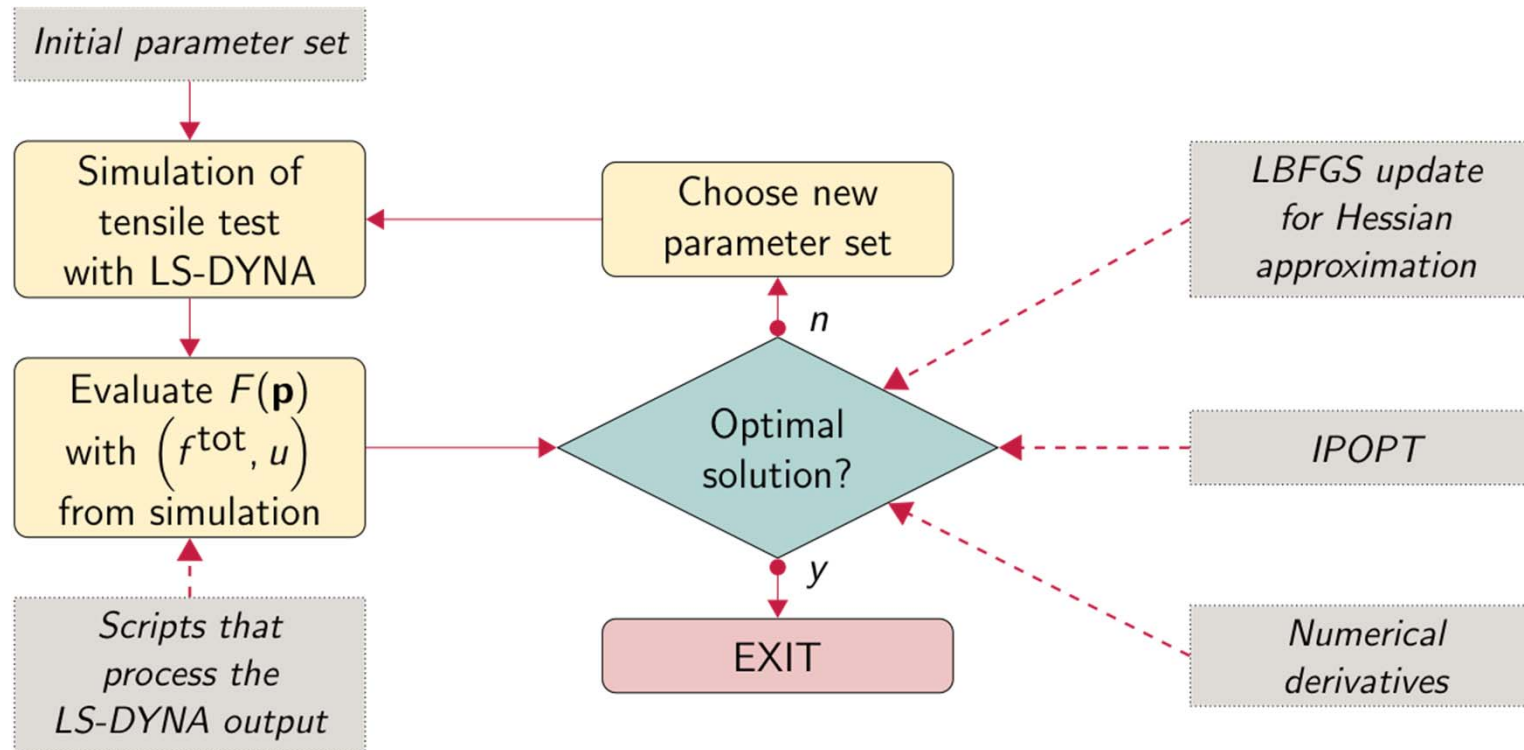


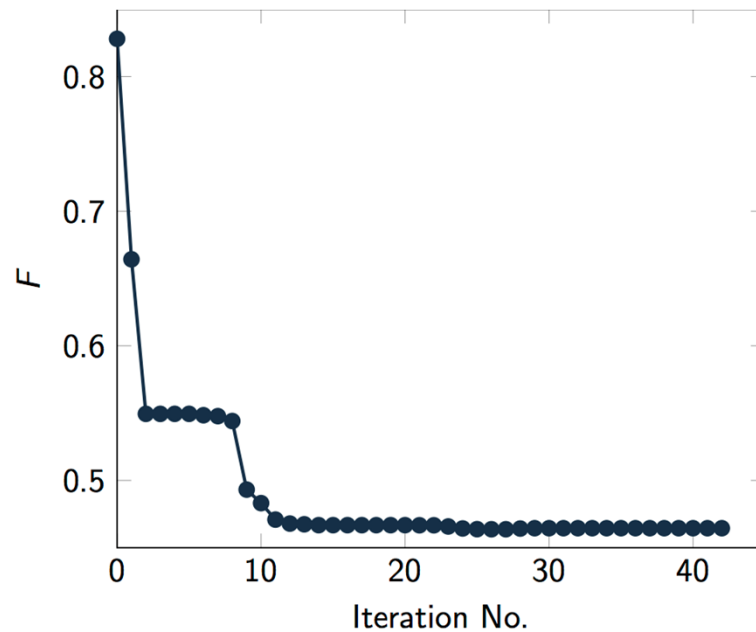
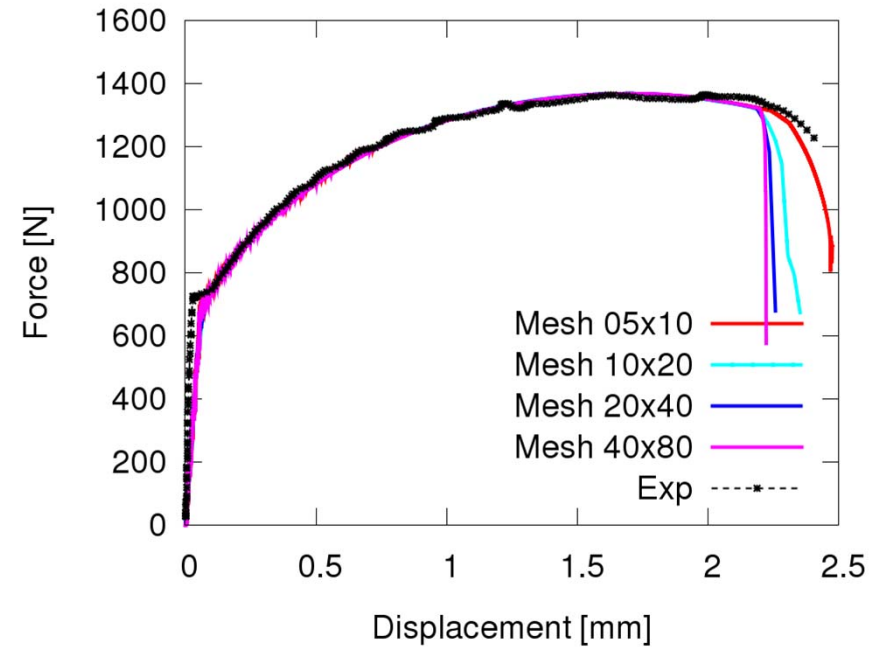
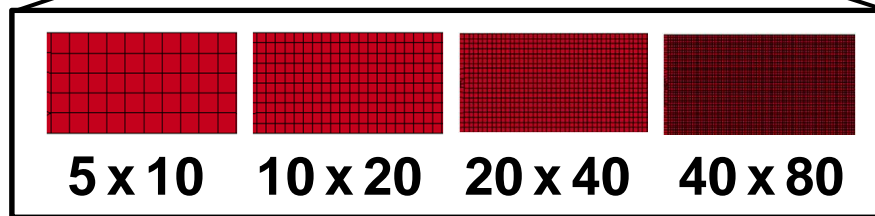
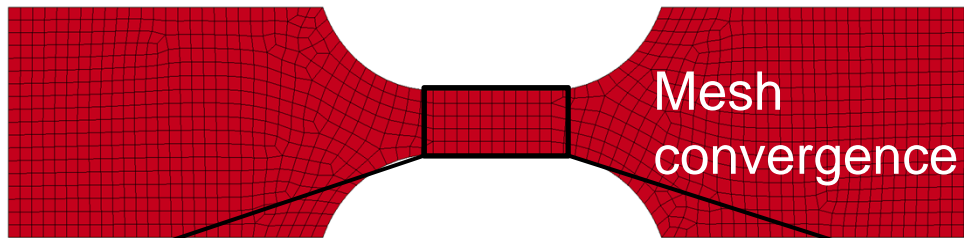
Experimental setup for determining the flow curves for varying strain rates

[Nordmetall]

- Parameter identification based on experimental data
- Non-linear objective function to identify optimal parameter vector \mathbf{p}

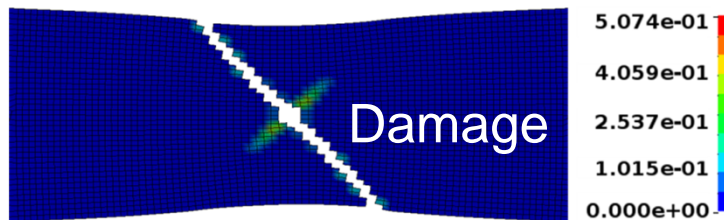
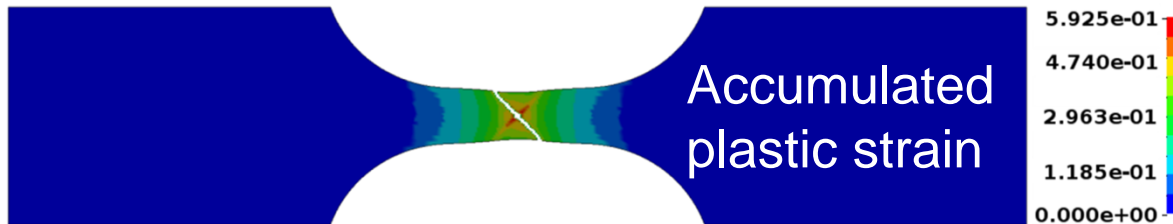
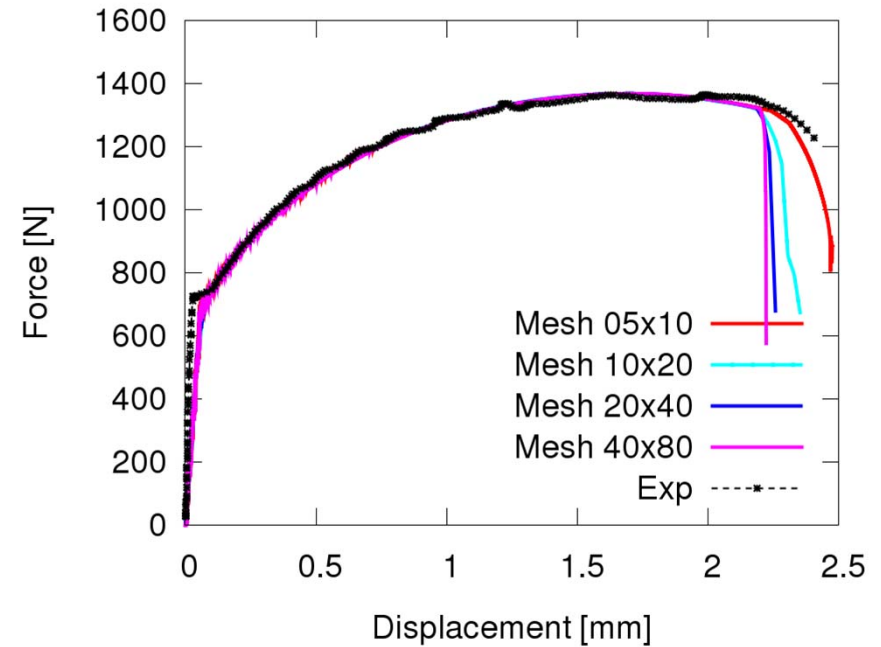
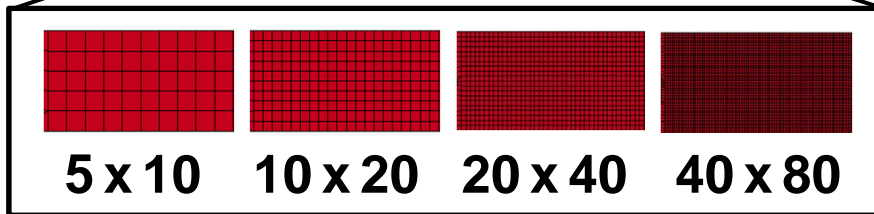
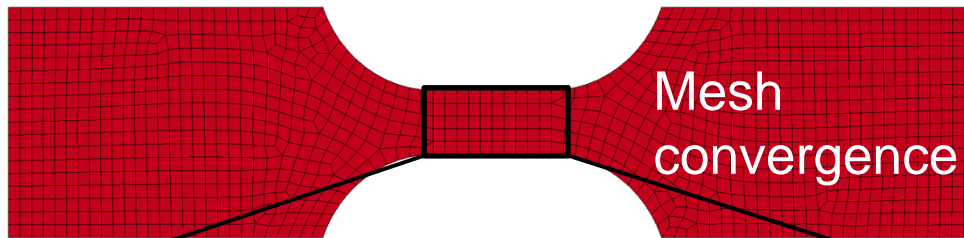
$$F(\mathbf{p}) = \frac{1}{2N} \sum_{i=1}^{N-1} (u_{i+1} - u_i) [(f_{i+1}^{tot}(\mathbf{p}) - \tilde{f}_{i+1}^{tot})^2 + (f_i^{tot}(\mathbf{p}) - \tilde{f}_i^{tot})^2]$$

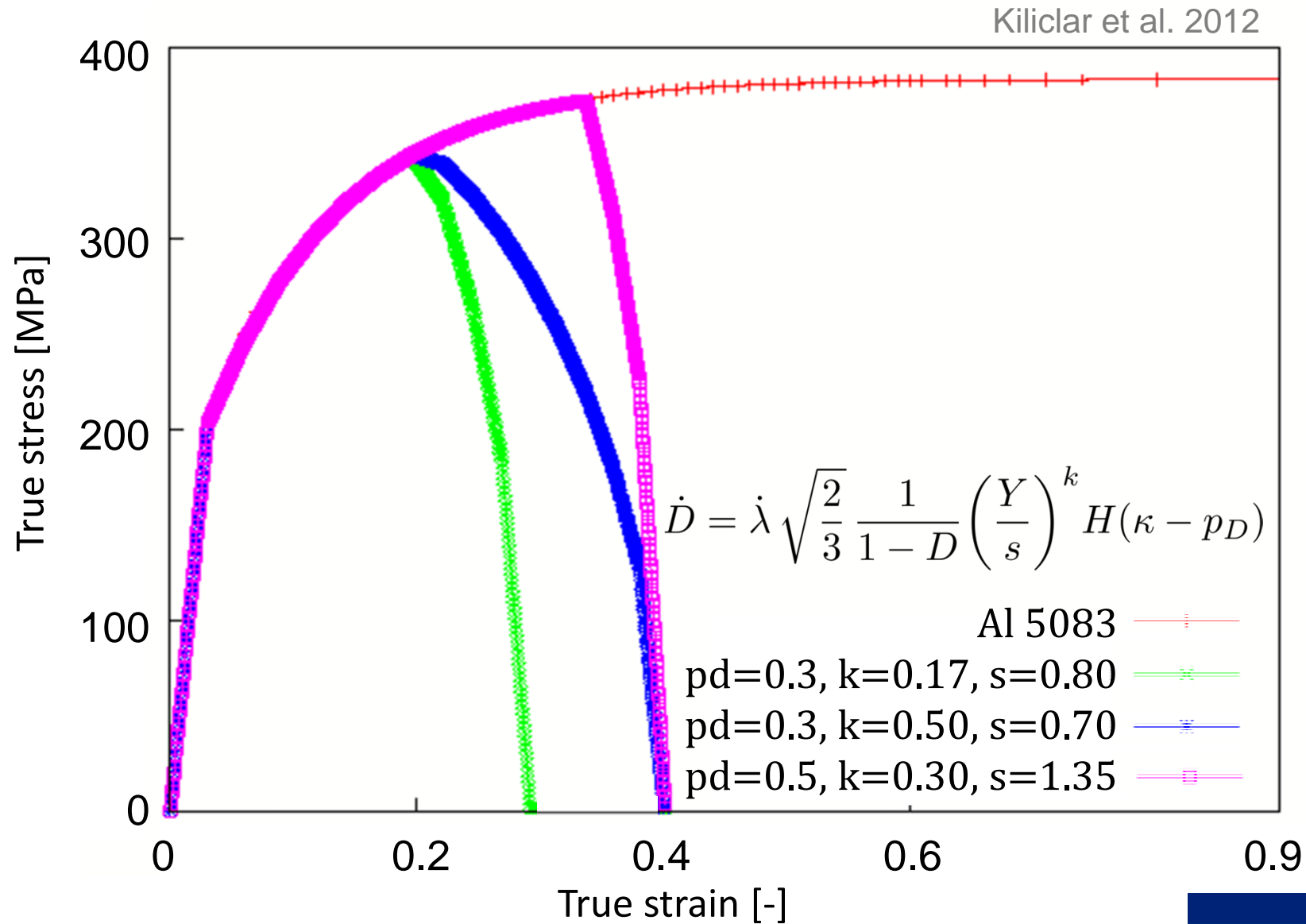




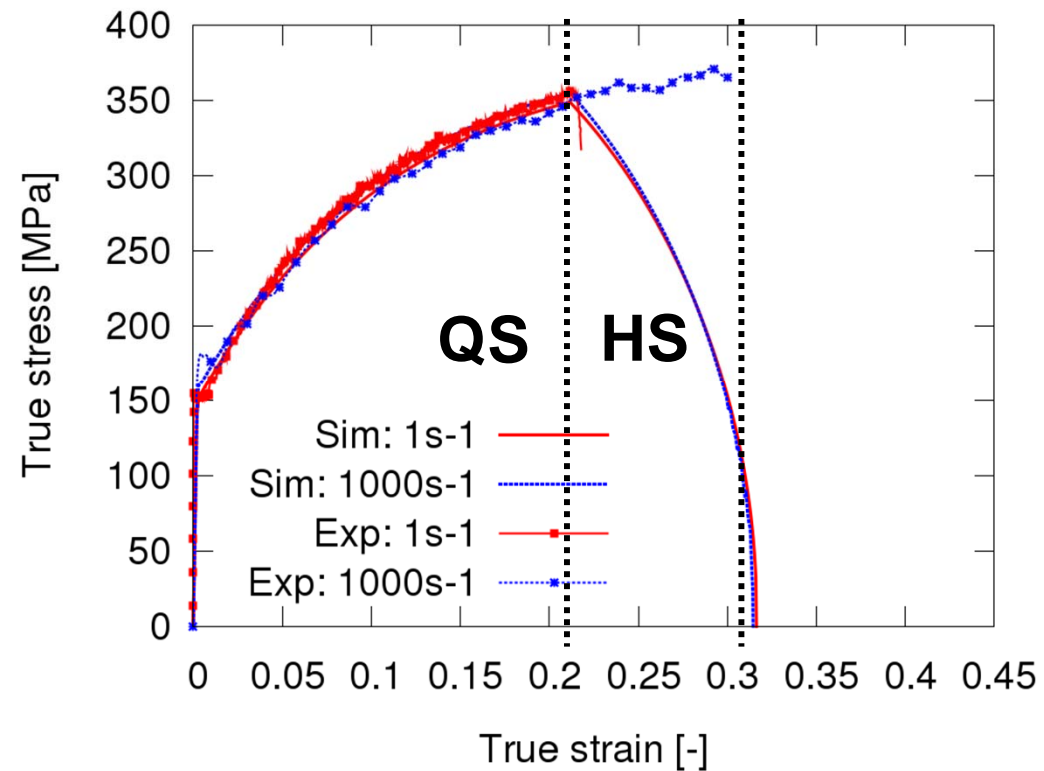
- Optimization by IPOPT works fine
- Good matching of experiment and simulation
- Localization problem

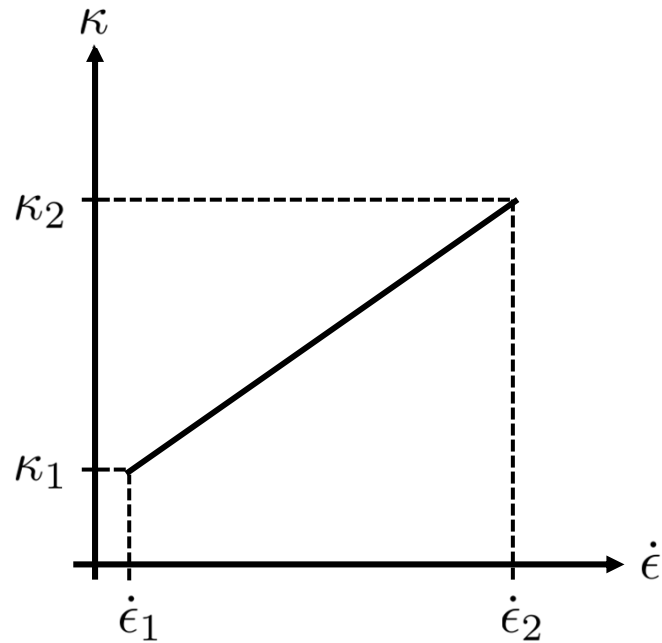




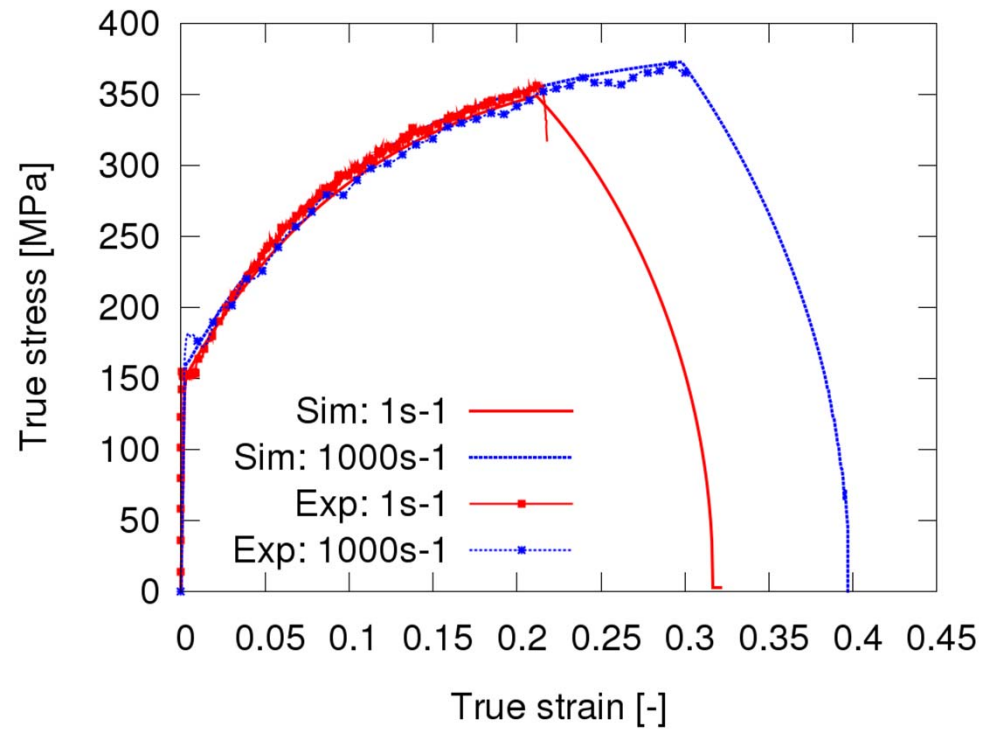


- Aluminum EN 5083
- Negligible strain rate sensitivity by means of higher stress level
- Higher formability with increasing strain rate

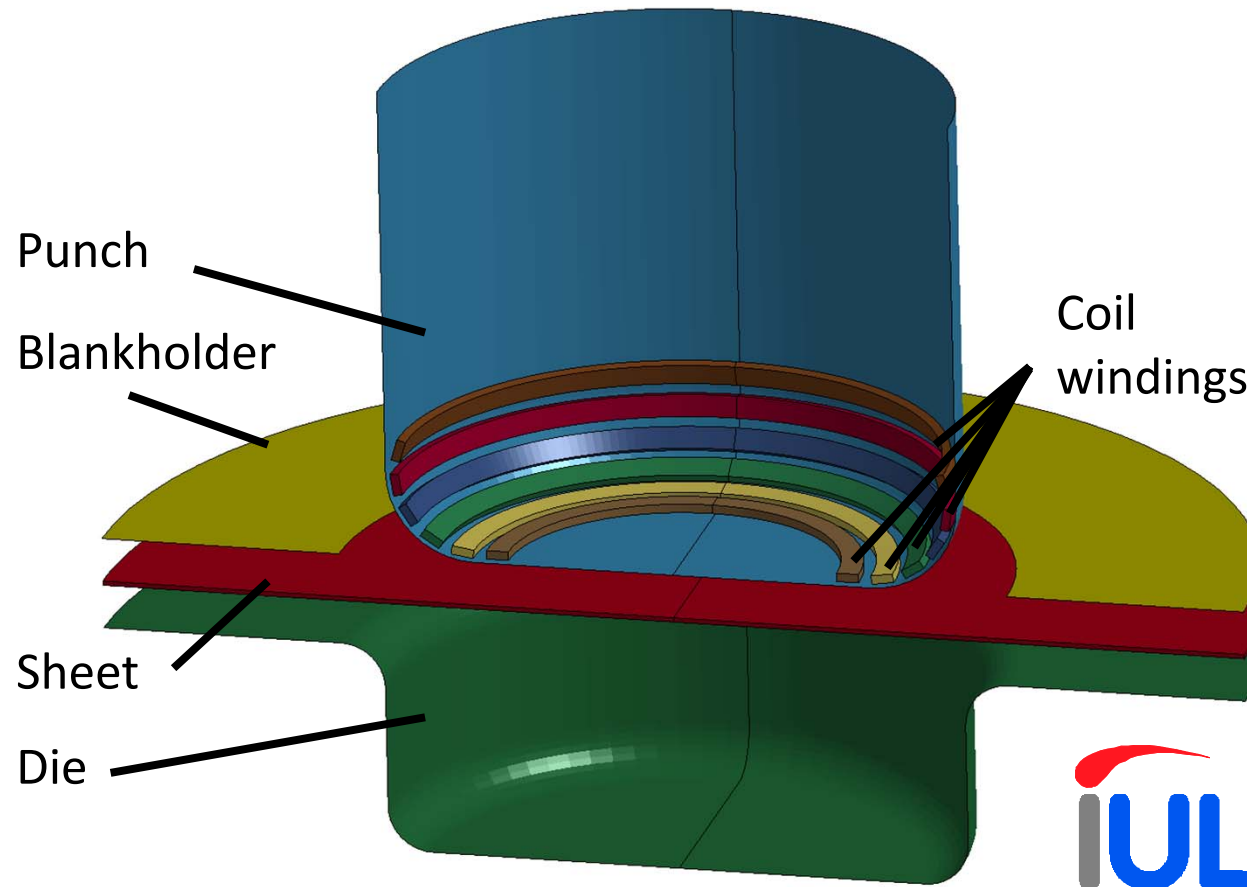




$$p_D = \kappa_1 + \frac{\kappa_2 - \kappa_1}{\dot{\epsilon}_2 - \dot{\epsilon}_1} (\dot{\epsilon} - \dot{\epsilon}_1)$$



- Rate dependent (linear) damage threshold
- Damage initiation is shifted

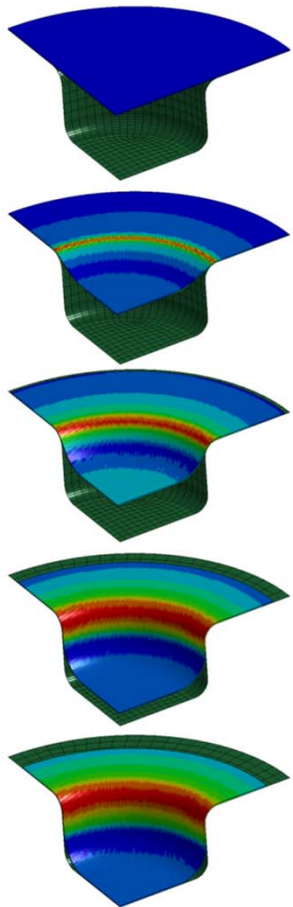


- Full coupled quasi-static and electromagnetic forming process

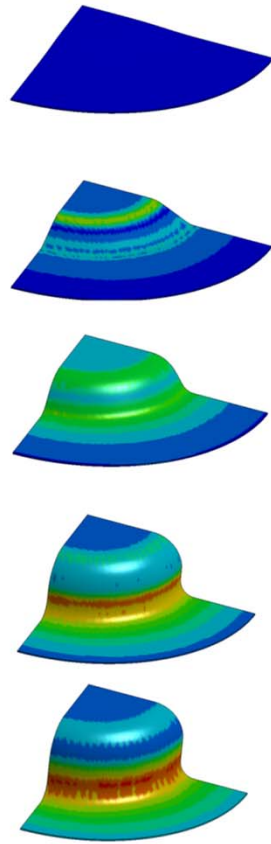


Deep drawing

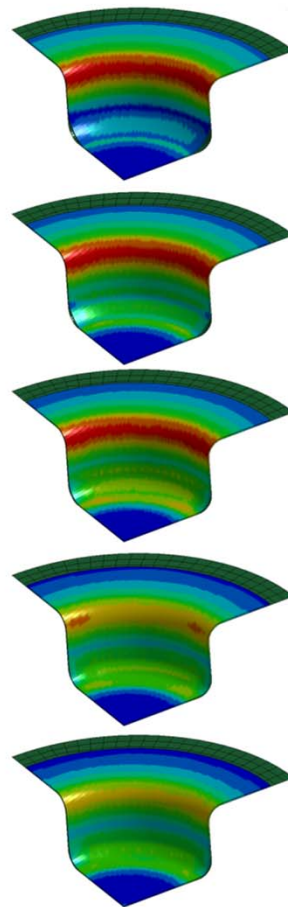
Electromagnetic forming



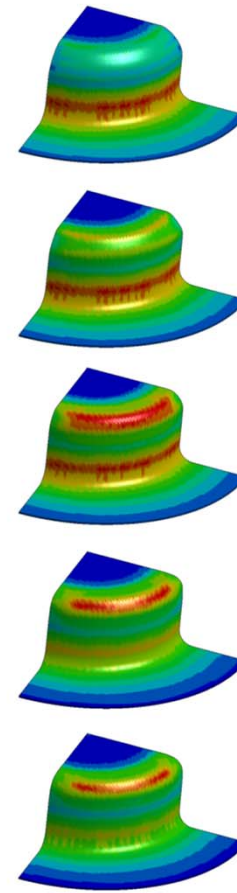
Top view



Bottom view



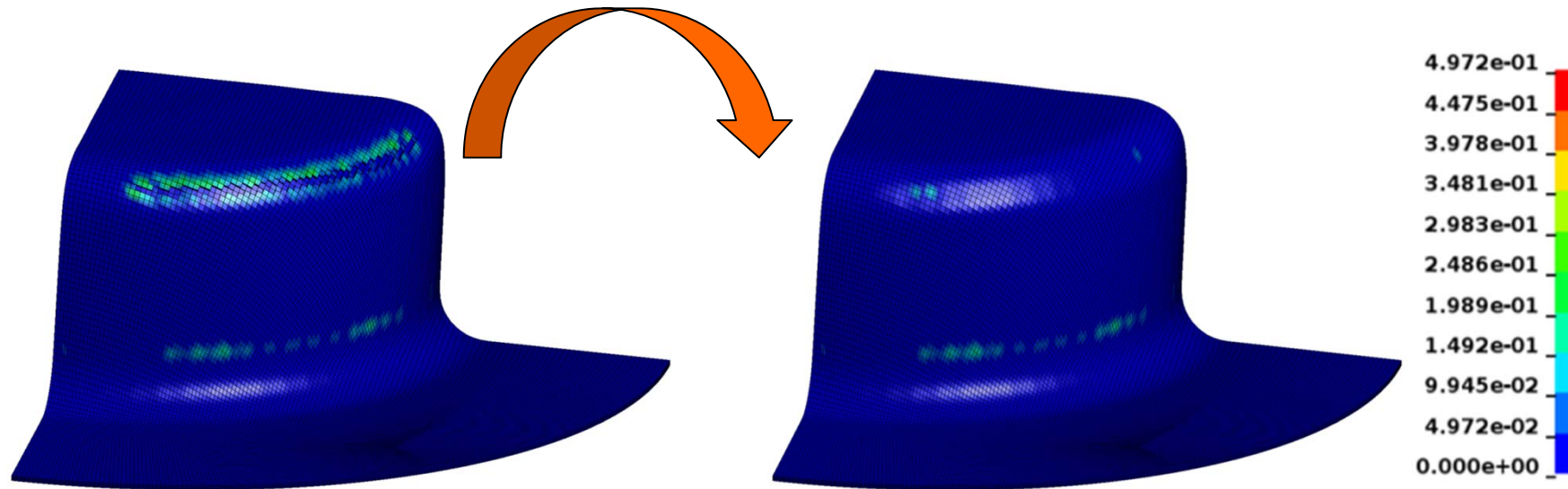
Top view



Bottom view

- Critical zone is in upper flange while deep drawing
- Critical zone moves to bottom radius while EM forming

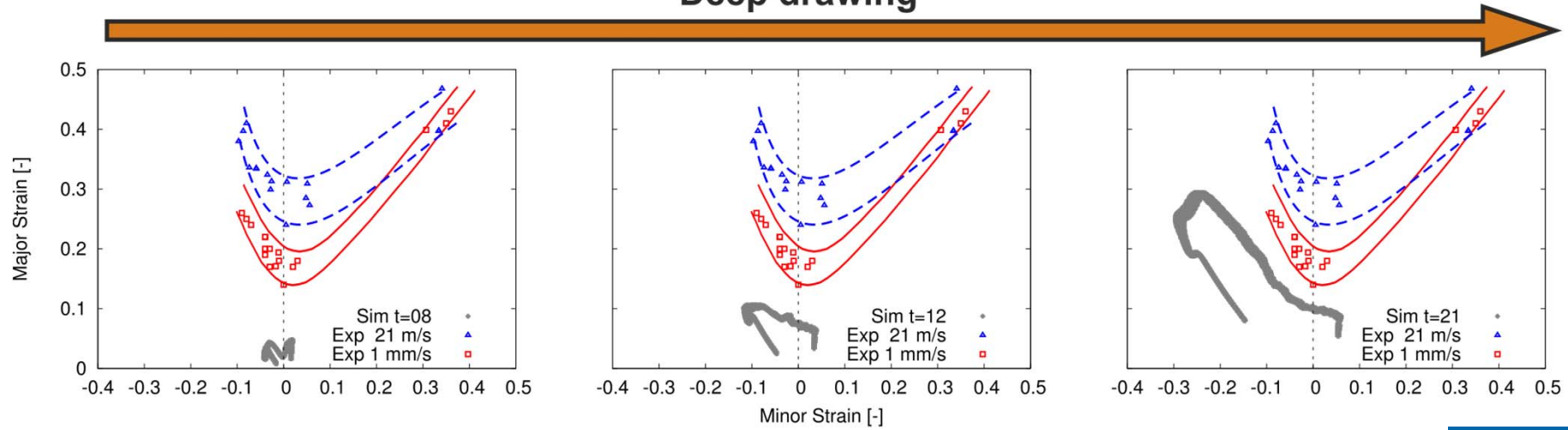
Extension of damage model



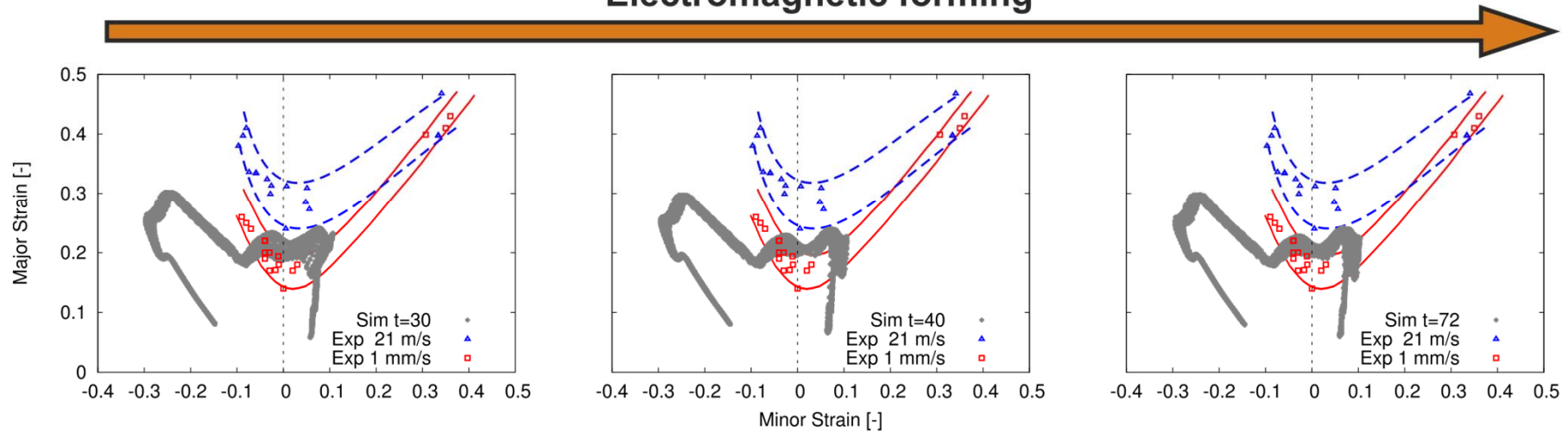
- “Crack” occurs during EM forming
- No further forming process is possible

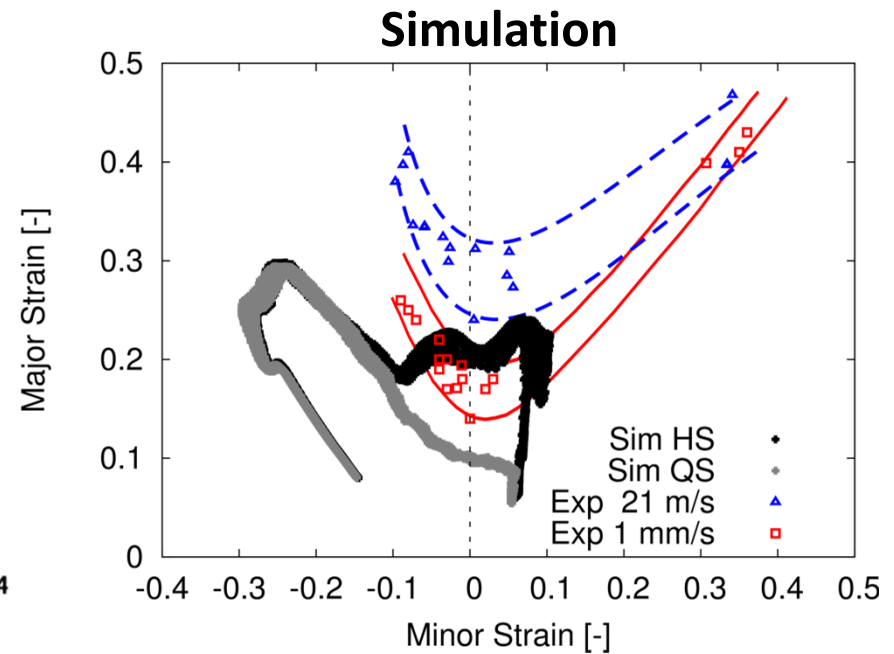
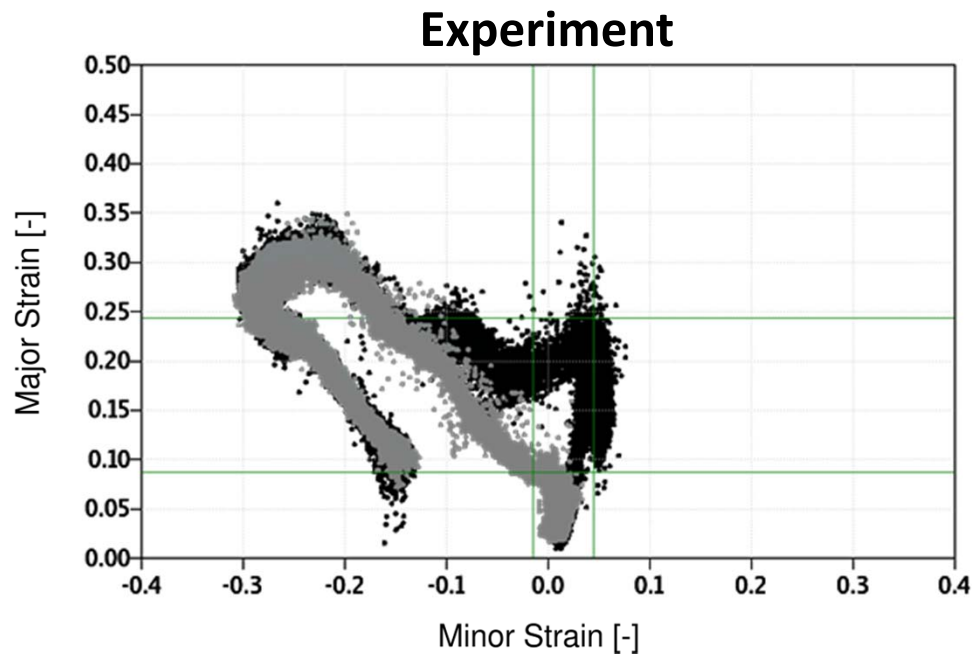
- Damage continue evolving but do not lead to failure
- Good agreement with experiments

Deep drawing



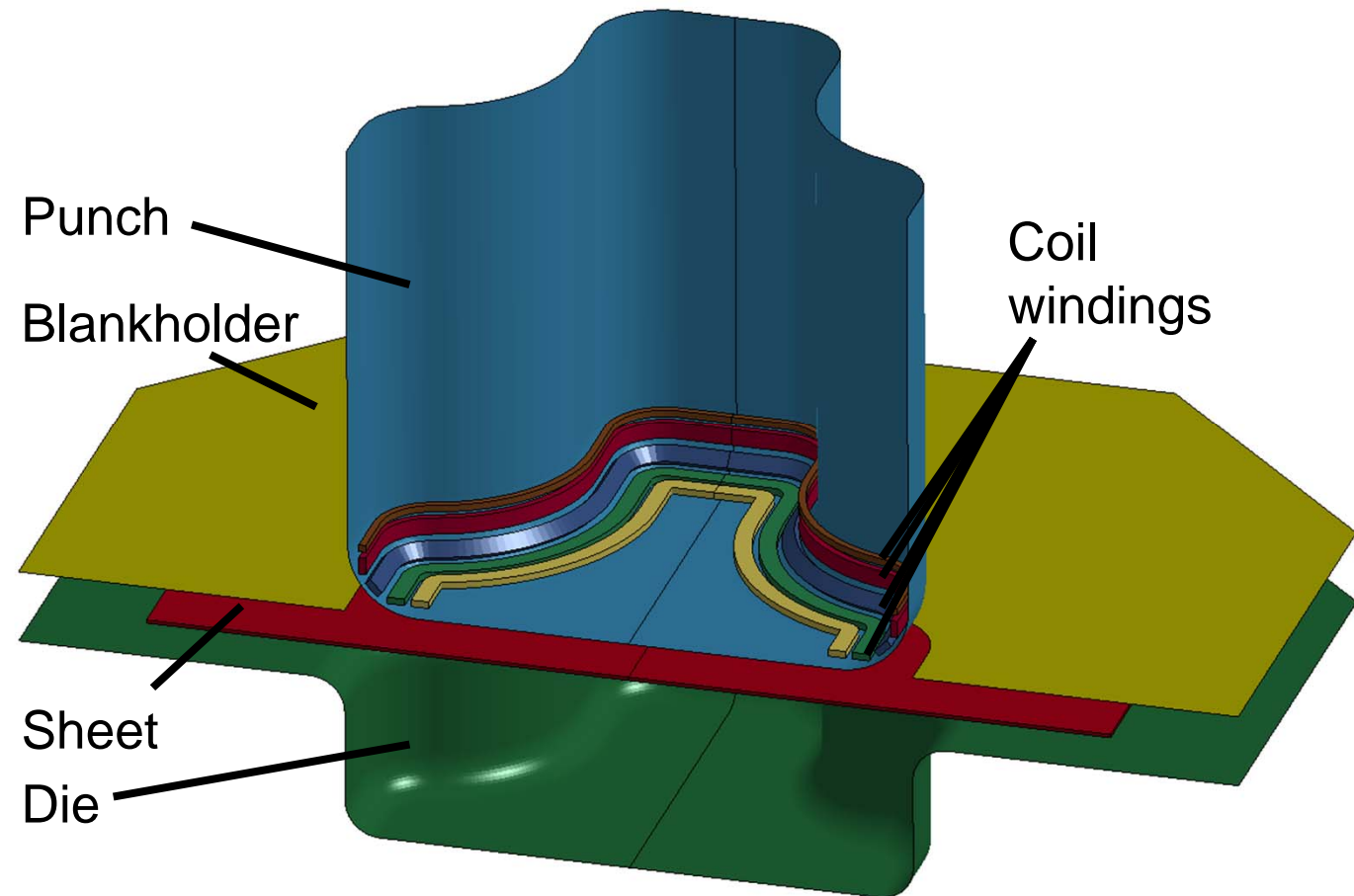
Electromagnetic forming





Kiliclar et al. 2015

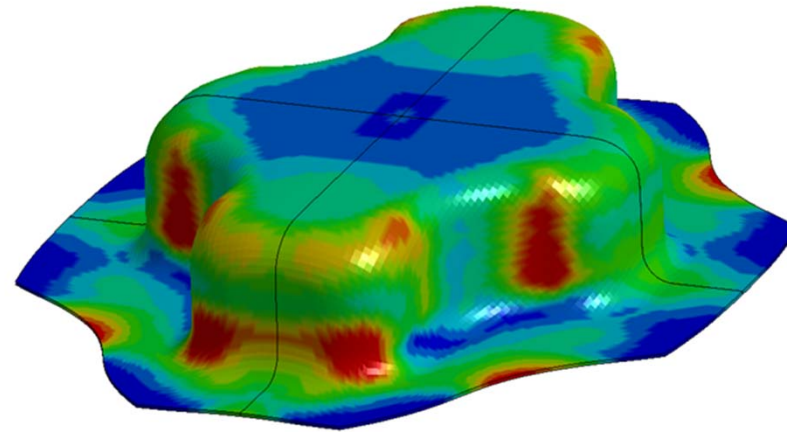
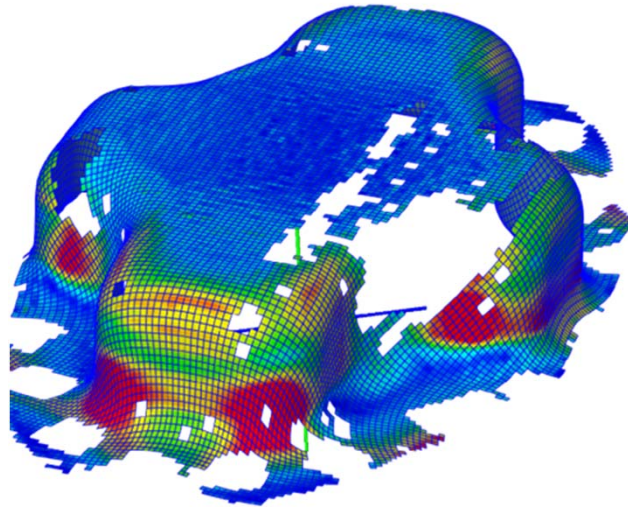
- Strain ratio exceeds QS-FLC during high-speed forming
- Good prediction of the overall material behavior
- Quantitatively good agreement with experimental result



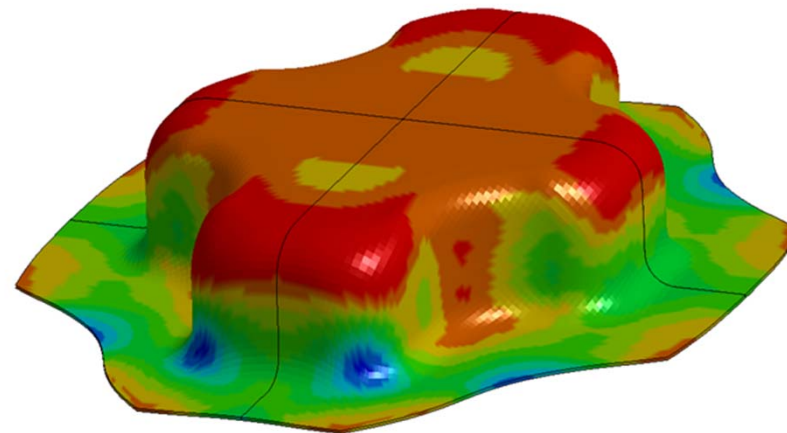
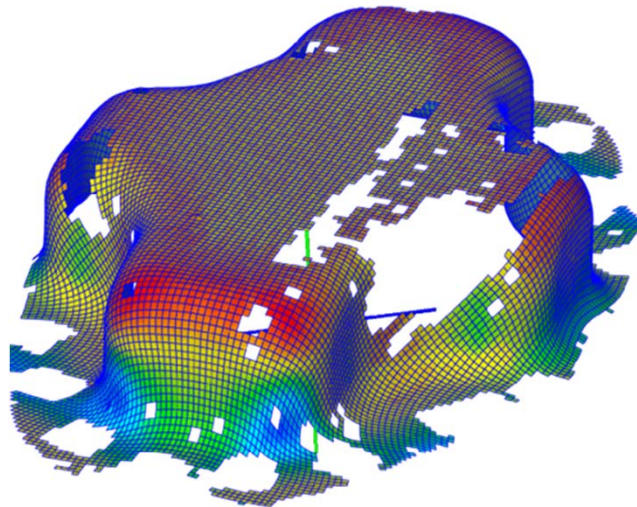
Experiment

Simulation

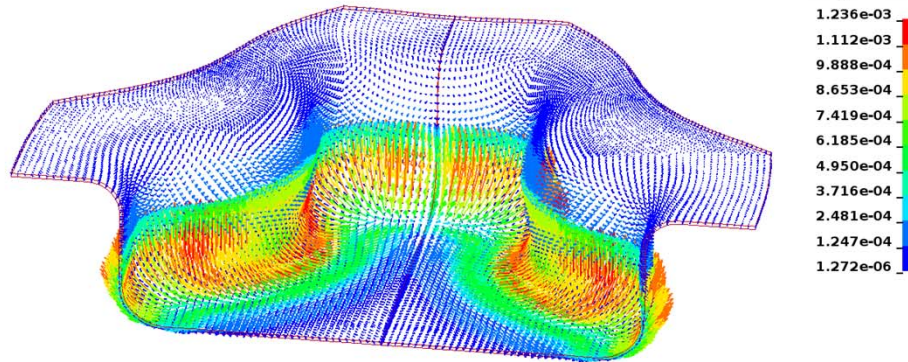
Major strain



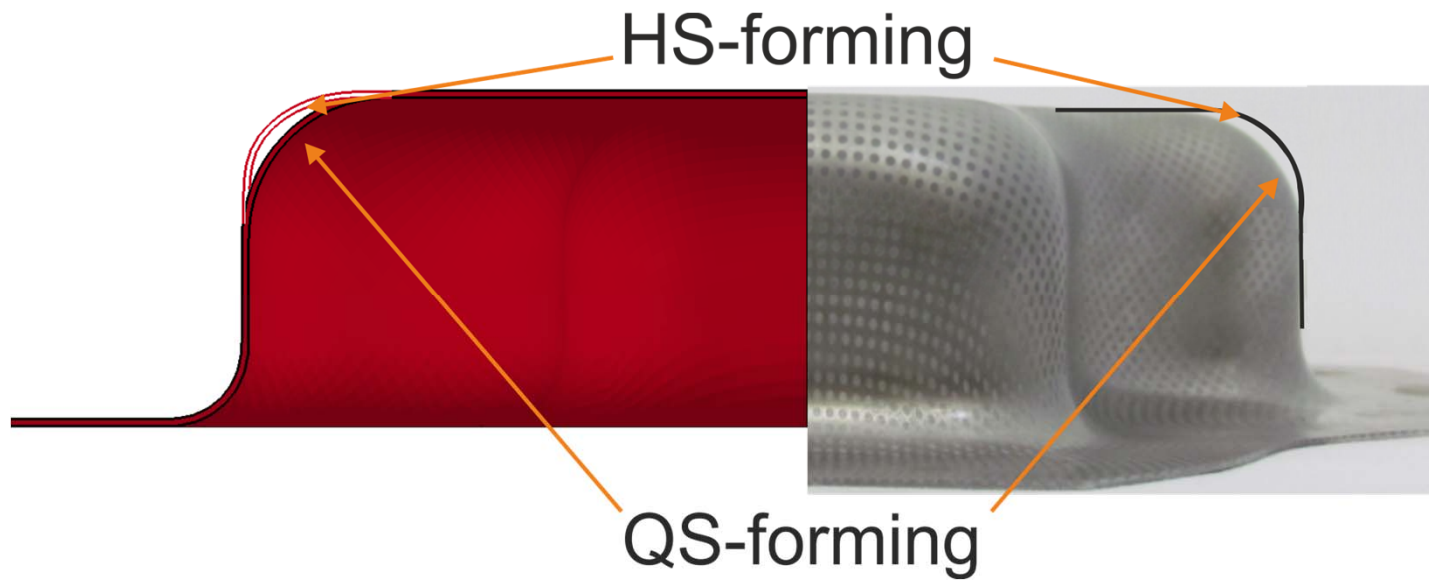
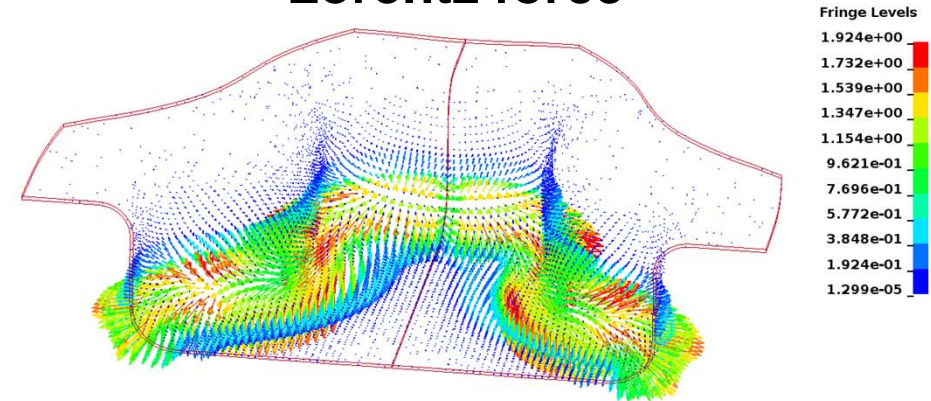
Minor strain

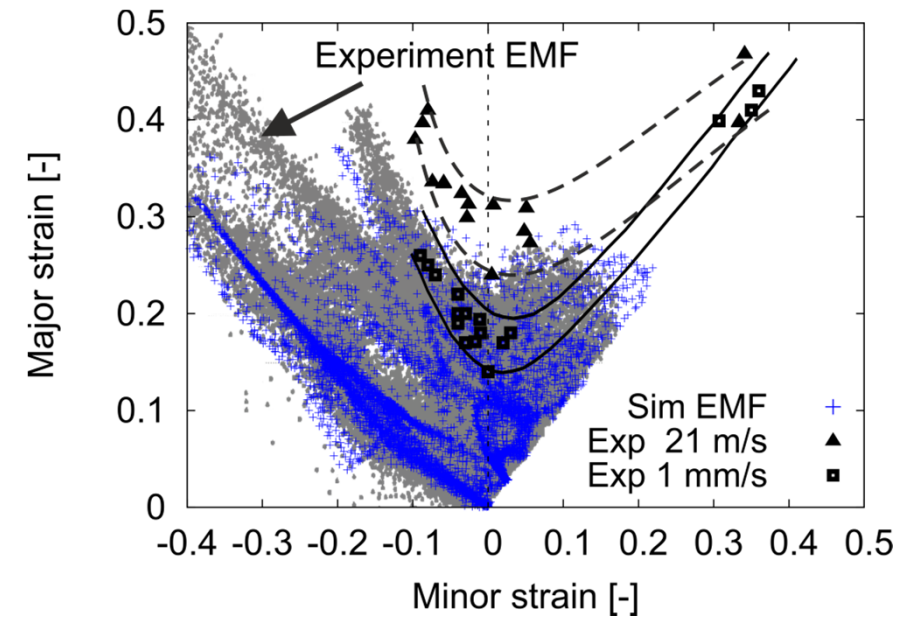
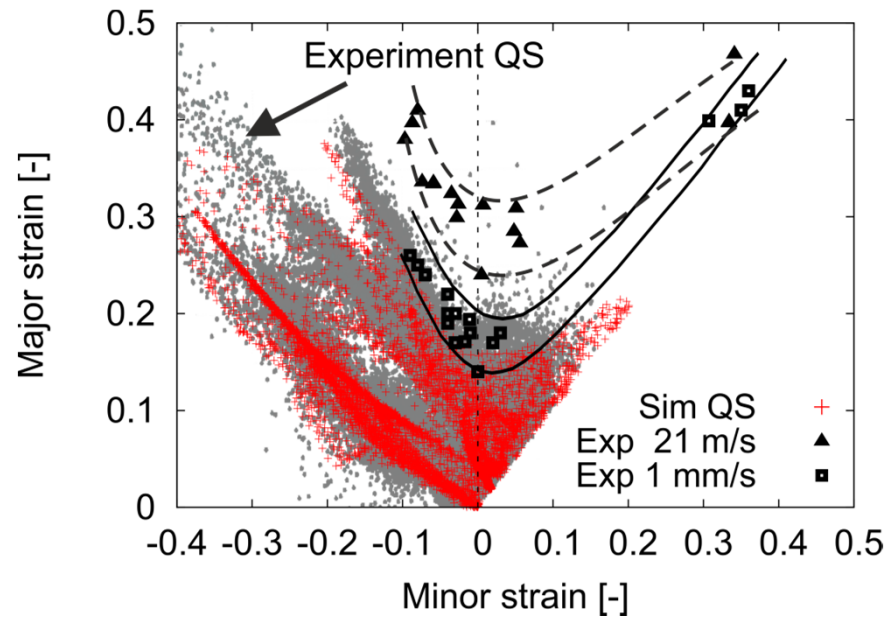


Magnetic field



Lorentz force





Kiliclar et al. 2015

- Strain ratio exceeds QS-FLD during high-speed forming
- Good prediction of the overall material behavior
- Qualitatively similarly to results of cylindrical cup

- Introduction of a framework for virtual process design in the context of combined quasi-static and electromagnetic impulse forming, featuring:
 - ✓ Suitable material model
 - ✓ Automatic parameter fitting based on experimental tensile tests
 - ✓ Good agreement between simulation and experiment
 - ✓ Realistic prediction regarding the combined forming processes
- First steps are taken, but:
 - ➔ Nonlocal formulations & anisotropic damage are current research tasks

Thank you for
your attention